Earth Syst. Dynam. Discuss., doi:10.5194/esd-2017-21, 2017
Manuscript under review for journal Earth Syst. Dynam.
Discussion started: 9 March 2017

Earth System Dynamics Discussions

A Lagrangian Perspective of the Hydrological Cycle in the Congo River Basin

Rogert Sorí[1], Raquel Nieto[1,2], Sergio M. Vicente-Serrano[3], Anita Drumond[1], Luis Gimeno[1]

[1] Environmental Physics Laboratory (EphysLab), Universidade de Vigo, Ourense, 32004, Spain
[2] Department of Atmospheric Sciences, Institute of Astronomy, Geophysics and Atmospheric Sciences, University of SãoPaulo, São Paulo, 05508-090, Brazil
[3] Instituto Pirenaico de Ecología, Consejo Superior de Investigaciones Científicas (IPE-CSIC), Zaragoza, 50059, Spain

Correspondence to: Rogert Sorí (rogert.sori@uvigo.es)

Abstract.

The Lagrangian model FLEXPART was used to identify the moisture sources of the Congo River Basin (CRB) and investigate their role in the hydrological cycle. This model allows us to track atmospheric parcels while calculating changes in the specific humidity through the budget of evaporation-minus-precipitation. The method permitted the identification at an annual scale of five continental and four oceanic regions that provide moisture to the CRB from both hemispheres over the course of the year. The most important is the CRB itself, providing more than 50% of the total atmospheric moisture income to the basin. Apart from this, both the land extension to the east of the CRB together with the ocean located in the eastern equatorial South Atlantic Ocean are also very important sources, while the Red Sea source is merely important in the budget of *(E-P)* over the CRB, despite its high evaporation rate. The moisture sink patterns over the CRB in air masses tracked forwards from all the sources follow a latitudinal rainfall migration and are mostly highly correlated with the pattern of precipitation rate, ensuring a link between them. The analysis of the wet and dry periods in the CRB confirms the key role of the basin in modulating the fresh water balance within the basin itself.

1 Introduction

The water falling on a given area as precipitation may have been supplied to it by local evaporation or transpiration, alternatively it may have been advected from a remote terrestrial source, or it may have originated in evaporation from the oceans (Dirmeyer, 1999). In recent years, a great number of studies have focused on deepening our understanding of these issues, particularly the mechanisms of water vapour transport in the atmosphere and the identification of moisture sources. These issues are considered some of the major challenges in the atmospheric sciences (Gimeno et al., 2013a). Several techniques and methods have been implemented in an attempt to address these matters; a summary of the main strengths and weaknesses of each was provided by Gimeno et al. (2012).

In respect of Africa in particular, some authors have investigated the sources of moisture for the whole continent (van der Ent., 2010; Gimeno et al., 2010, 2012), and specific regions such as the Sahel (Nieto et al., 2006; Salih et al., 2015; Keys et al.,

2012, 2014), Ethiopia (Viste and Sorteberg, 2013), and the wider region of West Africa (Savenije, 1995; Eltahir and Gong, 1996; Druyan and Koster). Nevertheless, the Congo River Basin (CRB), in the highly convective region of Central Equatorial Africa (CEA), is one of the least studied of the major global river basins (Alsdorf et al., 2016). Focusing on several world river catchments including the Congo, Stohl and James (2005) used the Lagrangian model FLEXPART over a period of 4 years (Dec 1999 - Nov 2003) to diagnose the net budget of *(E-P)*, where *(E)* denotes evaporation and *(P)* precipitation. However, the short time-scale involved in this study was not sufficient to investigate properly the variability and other aspects of the hydrological cycle over the CRB. Gimeno et al. (2010) argued that in tropical South Africa during the austral winter the rate of evaporation is so high that it provides moisture for most of the precipitation over the Congo, and besides this according to van der Ent et al. (2010), the moisture that evaporates in East Africa is the main source of rainfall in the CRB.

More accurate results on the evaporative moisture sources for the CRB, together with their seasonal variations and mean contributions over a period of 25 years, are available online from the Center for Ocean-Land-Atmosphere Studies (COLA). These were calculated using a Quasi-Isentropic method, an Eulerian approach implemented in Dirmeyer et al. (2009), and the results highlight that the main evaporative sources for precipitation lie within the basin itself, in addition to the land to the east of the basin along the oriental African coasts, and the Atlantic and Indian Oceans. However, it is not yet clear what the role of the CRB moisture sources is in other stages of the hydrological cycle and during extreme events in the basin. Most of the studies based on instrumental records in Africa indicate that droughts have become more frequent, intense and widespread during the last 50 years (Dai, 2013; Masih et al., 2014). The occurrence of drought is especially important in regions where economic activities are highly dependent on water resources (like the CRB), and particularly affect those African nations that are heavily reliant on agriculture (Lobell et al., 2011a, b).

The objectives of this study are: i) to identify the main continental and oceanic moisture sources for the CRB from a Lagrangian perspective and determine their role, including that of the basin itself in the total moisture influx to the basin, and ii) to investigate drought and wet conditions in the CRB and the relationship of these to atmospheric moisture influx.

1.1 Region of Study

The Congo River Basin (CRB) is located in central-equatorial Africa, an important part of the continent containing major rivers and dense forest. With an approximate area of 3,687,000 km^2 (Alsdorf et al., 2016), the basin includes several African countries: the Democratic Republic of the Congo (DRC), the People's Republic of the Congo, the Central African Republic, and parts of Zambia, Angola, Cameroon, and Tanzania (Chishugi, 2008). The Congo River (also known as the Zaire) is over 4,375 km long, considered to be the fifth longest river in the world, and the second longest in Africa after the Nile River (IBP, 2015). The CRB comprises the second largest continuous rainforest in the world, covering an area of approximately 1.8 Million km^2, being extremely important for storing carbon and having an impact on the global water cycle through local water recycling (Haensler et al., 2013). These moist forests are the continent's main forest resource, containing an extraordinary biodiversity (SCBD-CAFC, 2009) that brings important economic benefits to local communities (Hugues, 2011). Nevertheless, satellite

Earth Syst. Dynam. Discuss., doi:10.5194/esd-2017-21, 2017
Manuscript under review for journal Earth Syst. Dynam.
Discussion started: 9 March 2017

data show a widespread decline in greenness in the northern Congolese forest over the past decade, which is generally consistent with decreases in rainfall, terrestrial water storage, and other related aspects (Zhou et al., 2014).

The air masses originating from three permanent anticyclones located to the north-west (Azores), south-west (St. Helena), and south-east (Mascarene) of the CRB converge along the Intertropical Convergence Zone (ITCZ), which separates the southerly low-level winds from the northerly winds, and the Inter-Oceanic Confluence Zone (IOCZ), separating the westerly from the easterly winds in the southern part of Africa (Samba and Nganga, 2012). The rainfall-generating mechanisms are controlled by a zone of shallow depression systems in the Congo forest basin (Samba and Nganga, 2012) as well as north-south ITCZ migration (Samba and Nganga, 2012; Alsdorf et al., 2016) together with Mesoescale Convective Systems (MCS) (Jackson et al., 2009) and the African Easterly Jet (Nicholson, 2009; Pokam et al., 2012).

2 Data and Methodology

The analysis covers the period 1980-2010. The drainage area of the Congo River Basin (Figure 1) was defined using geo-referenced watershed boundaries on a 30 arc-second resolution map (a Hydrobasin product of HydroSHEDS (Hydrological data and maps based on SHuttle Elevation Derivatives at multiple Scales), Lehner and Grill (2013)). This was used to obtain the spatial mask of the basin, which was later implemented in the computations.

The methodology implemented here is based on the Lagrangian model FLEXPART developed by Stohl and James (2004, 2005). The model outputs were used to compute the gain and loss of humidity along tracks of air particles leaving and arriving in the CRB. The model allows us to track the parcels backwards and forwards, allowing the identification of the moisture sources for the CRB and then their climatological moisture supply and the relationship to the precipitation in it. The approach implemented here has been widely and successfully applied to study the atmospheric branch of the hydrological cycle (e.g., Stohl and James, 2004, 2005; Nieto et al., 2008; Gimeno et al., 2010; Gimeno et al., 2012; Chen et al., 2012; Viste and Sorteberg, 2013; Drumond et al., 2014).

In this method, the atmosphere is divided into N evenly distributed “particles” or “parcels”, whose advection is described by Eq. (1):

$$dx/dt = v\,[x(t)], \quad (1)$$

where x is the position of the parcel and $v\,[x(t)]$ is the wind speed interpolated in space and time. The gain (through evaporation from the environment e) or loss (through precipitation p) of specific humidity (q) by each parcel is calculated following Eq. (2). Along individual trajectories q fluctuations can occur for nonphysical reasons (e.g., because of q interpolation or trajectory errors), a limitation partly compensated by the presence of so many particles in an atmospheric column over the target area, thus:

$$(e - p) = m(dq/dt), \quad (2)$$

where additionally m is the mass of a particle. By integrating over an area of interest it is possible to obtain the net effect of the moisture changes in all the particles in the atmospheric column and, as a consequence, a diagnosis of the surface freshwater flux, hereafter represented by *(E-P)* (Stohl and James, 2004). It is worth mentioning that in some regions atmospheric moisture is not precipitated but just flows through, while in others the convergence of moisture ensures that precipitation occurs (Pokam et al., 2012). A region is then considered a moisture source when *(E-P)>0*, and the net moisture budget of the particles tracked is favourable to evaporation from the environment to the particles. In moisture sink regions the opposite occurs, i.e., the associated moisture budget is favourable to moisture loss from the tracked particles to the environment. A analysis backwards in time tells us where the atmospheric moisture in the air masses over the CRB came from, enabling us to identify the main oceanic and continental sources of moisture. The analysis was applied for 10 days, which is the average residence time of water vapour in the atmosphere (hereafter we use *(E-P)i10*) (Eltahir and Bras, 1996; Numaguti, 1999).

The Lagrangian data used in this work were obtained from a FLEXPART v9.0 experiment executed on a global domain, in which the atmosphere was divided into about 2.0 million uniformly distributed particles. FLEXPART uses ERA-Interim reanalysis data (Dee et al., 2011) available at 6 h intervals (00, 06, 12, and 18 UTC) at a resolution of 1° at 61 vertical levels, from 0.1 to 1000 hPa, with approximately 14 model levels below 1500 m and 23 below 5000 m. This is important because the transport of water vapour occurs mainly in the lower troposphere, which is clearly affected by the earth's topography (Peixoto and Oort, 1992).

To ensure the selection of the most important annual moisture source regions for the CRB, a threshold was used to delimit these, defined by the value of the 90th percentile calculated from the annual *(E-P)>0* values integrated over the 10 days of transport. This value acts as boundary to delimit those regions where air masses gain more humidity on their journey to the CRB, representing the 10% of grid points with the highest positive values of *(E-P)i10* on the map. This criterion was applied for similar purposes by Drumond et al. (2014, 2016a, 2016b). The CRB itself is also considered a source of moisture, and its role in recycling is therefore evaluated here. Tracking the air parcels forwards from each of the delimited moisture sources allows us to compare their contributions and thus the importance of each in the total moisture influx to the CRB.

Data for precipitation were obtained from the CRU TS v.3.23 database (Harris et al., 2014) with a spatial resolution of 0.5º. The runoff, the geopotential at 850 hPa, and the vertical integrated moisture flux (northwards and eastwards) form part of the Era Interim Reanalysis Project (Dee et al., 2011), with a resolution of 1ºx1º in latitude and longitude. The corrected monthly mean discharge of the Congo River recorded at the gauging station at Kinshasa (4.0º S, 15.3º E) was provided by the Global Runoff Data Centre (GRDC). To estimate the total evaporation over the moisture sources we use two state-of-the-art base data sets: OAFLUX and GLEAM. The monthly ocean evaporation data are obtained from the OAFLUX project, which uses surface meteorological fields derived from satellite remote sensing and reanalysis outputs produced from the NCEP and ECMWF models (Yu et al., 2008). The monthly evaporation from the land is estimated from GLEAM (Global Land Evaporation

Amsterdam Model) data, which takes into account a set of algorithms including transpiration, bare-soil evaporation, interception loss, open-water evaporation and sublimation (Miralles et al., 2014), all of which are important considering the dense forests of the CRB.

The role of general circulation in the hydrological cycle can be shown clearly through maps of vertically integrated atmospheric moisture flow (Peixoto and Oort, 1992). Also known as Vertically Integrated Moisture Flux (VIMF), this allows readers to compare moisture transport under an Eulerian perspective (Drumond et al., 2014); consequently these maps should lend support to explanations of moisture budget calculated using FLEXPART.

The methodology used to quantify drought or wet conditions in the CRB is based on the Standardized Precipitation Evapotranspiration Index (SPEI), which is a multi-scalar drought index that considers the effect of both precipitation and atmospheric evaporative demand (AED) (Vicente-Serrano et al., 2010). The SPEI for the CRB was calculated at time scales from 1 to 24 months using precipitation and reference evapotranspiration (ETo) obtained from the CRU TS v.3.23 dataset. The criterion of McKee et al. (1993) was used to identify those years of severe and extreme drought and wet conditions (according to the SPEI threshold of +/-1.5). Hydrological drought conditions were quantified at the gauging station of Kinsasha using the Standardized Streamflow Index (SSI) (Vicente-Serrano et al., 2012).

3 Results and Discussion

3.1 Climatology: Rainfall and runoff over the basin and Congo River discharge

The annual cycle of precipitation over the CRB is depicted in Figure 2. The most notable feature of the monthly patterns is the latitudinal migration of the precipitation maximum throughout the year, which leads to different seasonal patterns over the territory according to Chishugi (2008). Nevertheless, the evaluation of the impact of rainfall on various sectors and its distribution throughout the annual cycle may be as important as the total annual rainfall (Owiti and Zhu, 2012). During January, February and March, the southern half receives more precipitation, while April is a transitional month with maximum rainfall in the west-central and northeast parts of the basin. From May to August the rainfall pattern appears homogeneous and reveals that the majority of the average precipitation occurs in the northern part, coinciding with the northward excursion of the ITCZ between February and August (Nicholson and Grist, 2003; Suzuki, 2011). In September the rainfall increases to the south affecting the centre of the basin, with the greatest extension in October. In November, the central and southwestern parts of the CRB receive more rainfall and during December there is also an extension to the southeast. The regime of precipitation over the CRB is clearly differentiated by a latitudinal oscillation of maximum accumulated values, in accordance with Alsdorf et al. (2016).

Monthly average precipitation shows an annual cycle with two maximum peaks during March-April and October-December, with values greater than 4.5 mm day^{-1}, each accounting for 21% and 32.6% of the mean annual rainfall in the CRB, respectively (Fig. 3). During June and July the average rainfall reaches its lowest level of around 2 mm day^{-1}. This cycle is similar to that

described by Washington et al. (2013), who compared the Congo rainfall climatology through several datasets obtained from reanalysis and ensemble models. However, they argued that the maximum rainfall in the basin occurs from March to May and from September to November, while the minimum occurs in June-August. The differences in monthly average precipitation may be due to the areas used; they used a box region over equatorial west Africa while we use the CRB boundaries.

The mean annual cycle of runoff in the CRB (Fig. 3) follows the same annual cycle as rainfall although it is always lower, varying between maximum values of 3.0 and 3.5 mm day^{-1} during November-March and minimum values below 1.5 mm day^{-1} during July and August.

The long-term distribution of precipitation and runoff over the African continent is almost the same (Siam et al., 2013), but the highest values of runoff are concentrated in the heart of the equatorial forest along the Middle Congo River branch (Alemaw, 2012), with these wetlands receiving the majority of their waters from upland runoff (Lee et al., 2011). The interannual correlation calculated between the two series over the CRB is high, r = 0.73 (significant at $p<0.05$) and r = 0.72 with a one-month lag. Fig. 3 shows that from March onwards the runoff reflects a one-month lag compared with precipitation. In general, in a steady state, the precipitation exceeds the evaporation (or evapotranspiration) over the land and the residual water runs off, resulting therefore in a continental freshwater discharge into the oceans (Dai and Trenberth, 2002). This also occurs in the CRB, where monthly values of precipitation minus the actual evapotranspiration obtained from the GLEAM dataset *(P-E)* seem to follow the same annual cycle as precipitation (Fig. 3). In June *(P-E)* has a negative value, which means that on average there is more evaporation in the basin than precipitation [as in Dai and Trenberth (2002) and Siam et al. (2013)]. The mean annual discharge of the Congo River is 38617.4 m^3 s^{-1}, as calculated from the GRDC monthly streamflow values registered at the Kinshasa-Brazzaville gauging station. The annual cycle of discharge (which is very similar to the precipitation and runoff) shows climatological maxima during November-December (Fig. 3) with values above 48000 m^3/s, while in July and August the minimum is less than 30000 m^3/s. Despite this, a difference is seen during March when high precipitation and runoff occur, but the discharge is low. During the next few months the precipitation and runoff decrease while in contrast the discharge increases, reaching a maximum in May. This lag reflects the time needed for the surface runoff to reach the river mouth (Dai and Trenberth, 2002, 2008; Marengo 2005; Rwetabula et al., 2007), as documented by Materia et al. (2012) using data recorded at Brazzaville station, about 400 km upstream of the river mouth. The direct relationship between precipitation over the basin and the discharge has a correlation of 0.52, which increases to 0.66 for a one-month lag (both statistically significant at $p<0.05$), confirming the lagged response mentioned earlier.

3.2 Identification of the moisture sources

In December, January and February over the CRB, areas of *(E-P)i10>0* (moisture sources) are represented by reddish colours, and are located over the northern half of the CRB and over the river mouth (Fig. 4). Negative values *(E-P)i10<0* (sinks), in blueish colours, cover the southern part of the CRB. Outside the boundaries of the CRB, *(E-P)i10>0* values can be seen spread

over the northeast of the continent, the Mediterranean Sea, the Red Sea, the Arabian Sea, and the tropical-east South Atlantic Ocean. Negative values are observed in the southeast of the basin, the tropical-west Indian Ocean, and the equatorial Atlantic Ocean around the Equator. For these three months the moisture convergence over central-equatorial Africa between 0º-20ºS, together with a divergence belt to the north of 0º, can be seen. The patterns of atmospheric divergence and convergence are associated with high-pressure systems as well low pressures at the Equator and in the ITCZ zone, approximately. The deep convection of the ITCZ depends on the contribution of water vapour by the surface moisture flux, supplied as surface latent heat flux, and the horizontal moisture flux in the lower free atmosphere (Suzuki, 2011). The Vertically Integrated Moisture Flux (VIMF) identifies moisture reaching the CRB from divergence zones in the Sahel and the Arabian Sea. It is extremely important to assess the VIMF because in Equatorial Central Africa the seasonal variability of the spatial gradient of precipitation recycling is regulated by both the direction and the strength of the moisture flux (Pokam et al., 2012).

In March the pattern of *(E-P)* changes over the basin, with the establishment of intense moisture sinks located to the centre-west. March seems to be a transitional month, and in April the pattern of *(E-P)* undergoes a more obvious change characterized by moisture loss over the northern half of the basin, a region that acts as a source in the months before this. Despite this, in both months the VIMF remains flowing from west to east over the basin, meanwhile the fields of convergence and divergence of moisture flux are not that different from previous months, instead highlighting a decrease in the divergence over the Arabian Sea (Fig. 4).

Just as in April, from May to September the budget of *(E-P)* over the basin is characterized by negative values in the northern half, in agreement with the maximum precipitation rates for these months (see Fig. 2). Specifically for June to August (the driest months) these values are confined to the northern part of the basin, while an evaporative condition prevails over the rest of the CRB. This demonstrates the ability of FLEXPART to simulate moisture losses in the basin associated with convective precipitation, as well as rainfall migration.

Beyond the CRB, from May to September the source areas *(E-P)i10>0* over the Arabian Sea diminish and the VIMF changes from its previously southwestward direction, which means that moisture transport from this region to Africa is no longer favoured. The *(E-P)i10* patterns are very similar to those of previous months for the other regions. During these months, in the equatorial Indian Ocean the moisture sinks are less intense than in previous months. At the same time a latitudinal displacement of moisture convergence and divergence zones occurs over central-equatorial Africa; a joint analysis of the maximum precipitation and convergence of the VIMF provides a rough estimate of the position of the ITCZ (Žagar et al., 2011).

Locations where *(E-P)i10>0* are generally accompanied by moisture flux divergence. However, the Arabian Sea supplies moisture to the CRB from May to October (blueish colour in the left-hand panels); specifically during June-September the VIMF shows an anticyclonic circulation over the Indian Ocean, which induces an intense north-east flow from the Arabian Sea to the Indian Peninsula, in fact this is an important moisture source for Indian monsoon rainfall (Levine and Turner, 2012).

The sink regions cover almost the whole of the CRB in October and November, when the southeast Atlantic Ocean, the continental regions in the east and north of the basin, and the southwest Indian Ocean all act as moisture sources. A transition of the scheme of moisture source regions takes place in November when once again over the Arabian Sea the *(E-P)i10>0* values appear (Fig. 4). This coincides with the beginning of the summer in the southern hemisphere and the decay phase of the Indian monsoon. The VIMF illustrates the moisture transport from the source regions to an area to the south of 0º in central-equatorial Africa, which enhances the precipitation process over the CRB in accordance with the southward movement of the ITCZ over Africa.

The climatological annual backward average of 10-day integrated *(E-P)* obtained from the Congo River Basin is presented in Fig. 5, which thus summarizes the most important moisture sources for the CRB throughout the year. As discussed earlier the boundaries of the moisture sources regions were identified by imposing the 90th percentile (p90) threshold of the annual *(E-P)i10>0* values. This equates to 0.43 mm day^{-1}, denoted in Figure 5 by the dashed lines. Five continental (C) and four oceanic (O) moisture sources were defined (Fig. 6). The five continental regions are located as follows: central and northeastern Africa (C1), centre-west part of the continent on both sides of Equator and at the river mouth (C2), from the river mouth along the Atlantic coast (C3), the east of the CRB extending along the west coast of Africa from the north of Somalia and Ethiopia to approximately 20ºS (C4), and finally the CRB itself. The four oceanic sources are: the Red Sea (O1), the Arabian Sea (O2), the eastern part of the tropical-equatorial South Atlantic Ocean along the coast of Africa (O3), and finally the tropical west Indian Ocean (O4). Moisture source regions are not stationary, varying in intensity from year to year, and expected to change in the future (Gimeno et al., 2013b). In addition, their role may change given the high decadal- and century-scale variability of the African climate (Masih et al., 2014). Nevertheless, these source regions provide insight into the mechanisms by which atmospheric moisture transport takes place towards central equatorial Africa, and how these impact precipitation in the CRB. A combination of factors may influence the role of each in the moisture influx into the CRB, such as the amount of water evaporated, the distance between each source and its target area, the atmospheric circulation, and the residence time of water vapour in atmosphere.

A comparison with the evaporative moisture sources for the CRB obtained using the quasi-isentropic method and available online (http://cola.gmu.edu/wcr/river/basins.html) confirms the importance of recycling in the CRB, in agreement with our results (Fig. 4, 5). There are nevertheless some differences at the annual scale, in that parts of the northern half of the basin act as moisture sinks (Fig. 5), and that the quasi-isentropic climatology mentioned above considers the entire basin to be an evaporative source. Another clear difference is the Indian Ocean, where our results reflect more clearly the seasonal latitudinal migration of the evaporative regions over the year.

3.3 Freshwater evaporation in the sources

An analysis of the evaporation rate over the moisture sources may support our understanding of their role in the moisture uptake in the CRB over the year. It is most important to note that although the total evaporation over a region considered to be

a moisture source, quantified here using GLEAM and OAFLUX, can be high, its contribution over the CRB might not be, because it could be providing moisture for precipitation in other target regions as well. The geographical location of the basin allows it to receive moisture from the Atlantic and Indian Oceans, as well from land regions around the basin, as Fig. 6 shows. Oceanic evaporation is highly important if we consider that evaporation from the ocean surface equates to roughly 84% of the total amount of water evaporated from the planet (Oki, 2005), and the role of the oceans is decisive in continental precipitation (Gimeno et al., 2010). The mean annual evaporation from the sources is given in Table 1 using data from OAFlux and GLEAM for the ocean and continental regions, respectively. On average, O4 and O1 are the most evaporative sources while O3 is the least evaporative.

Because the sources are located in two different hemispheres, they should have different annual evaporation cycles (Figure 7). From the FLEXPART backward experiment, monthly positive values of *(E-P)i10* were calculated over each source (hereafter E-FLEX) to compare over the year the evaporation from the sources with the moisture uptake from each source to the CRB. *(E-P)>0* can be discounted after *(E-P)* has been integrated without altering the general patterns of net precipitation, where *(E-P)>0* is discounted using a monthly or longer time scale (Castillo et al., 2014). In Figure 7 it is possible to observe both series for comparison, E-GLEAM (evaporation data over continental sources) or E-OAF (for oceanic ones) and E-FLEX. Starting the description with the most evaporative source, the O4 source is characterized by a maximum average E-OAF in May-July (>5.5 mm day^{-1}) and a minimum at the beginning and end of the year (Fig. 7, O4). This behaviour is in accordance with the results of Yu et al. (2007), who argued that the enhancement of evaporation occurs primarily during the hemispheric winter (defined as the mean of December–February for the northern hemisphere and June-August for the southern). The positive values of E-FLEX over this source (O4) are lower and quite different from the mean E-OAF during all months. This means that on average this source is not very efficient in supplying moisture to the CRB.

Nevertheless, the amount of moisture uptake from May to October is important if it is compared with moisture uptake over other oceanic sources, and it shows two peaks of E-FLEX: one in May and another in October, while it reaches minimum values during December-February (≤0.3 mm day^{-1}).

The second source with the major monthly E-OAF is O1 (4.60 mm day^{-1}), located on the Red Sea, where the oceanic evaporation rate is the highest in the world (Abdulaziz, 2012). After reviewing many studies Sofianos et al. (2002) confirmed several differences in the mean annual evaporation rate for the Red Sea, but it was estimated at around 2.06 m $year^{-1}$ (~5.6 mm day^{-1}). Figure 7 shows the annual cycle of evaporation (E-OAF) in this source, which is characterized by higher values during the boreal winter months and minimum values in summer, in accordance with Bower and Farrar (2015). Monthly E-FLEX values obtained over this source follow the same annual cycle as E-OAF but with lower values. As for O4, this means that the moisture contribution from O1 to the air masses in transit to the CRB is less than that which it provides itself to the atmosphere. In contrast it seems an important moisture source during December-February over continental areas to its Northeast and during June-August to the remote area of the Indian Peninsula (Gimeno et al., 2010).

Earth Syst. Dynam. Discuss., doi:10.5194/esd-2017-21, 2017
Manuscript under review for journal Earth Syst. Dynam.
Discussion started: 9 March 2017

The next region showing higher annual evaporative values (Table 1) is the continental source C2. The behaviour of this series differs from the previous two in that in this case the E-FLEX values are greater than the local evaporation calculated using the GLEAM dataset during February and from June to October (grey shaded areas in Fig. 7, C2). Despite the local evaporation E-GLEAM does not show any great variations over the year, varying from 2 to 3 mm day^{-1}, and the E-FLEX shows a bimodal cycle with a minimum in May (~0.2 mm day^{-1}) when major local evaporation occurs, and a maximum in August (~4.2 mm day^{-1}) when local evaporation is at its lowest. This behaviour illustrates that it is possible to have moisture available in the atmosphere (higher E-GLEAM values) but less humidity is taken up by air masses and then carried towards our target region (lower values of E-FLEX). This is the case during March to June, and the opposite occurs during July to October. The grey shaded areas in Fig. 7 indicate those months when the transport of moisture is favoured from the source to the CRB. Over the course of several days an air parcel may undergo multiple cycles of evaporation and precipitation (Sodeman, 2008) and in our case after integrating monthly data over 10 days it is hardly surprising that the E-FLEX values could be greater than local evaporation. Nevertheless, C2 is a land region, where the recycling concept is most useful because moisture for evaporation is limited by precipitation, whereas over the oceans the surface is clearly wet regardless of whether it rains or not (Trenberth, 1999).

One of the aims of this study is to determine the possible factors that inhibit or favour the transport of moisture from a specific source to the CRB. The efficiency of a region providing moisture for a target area depends on the amount of evaporated water that reaches it, and not just on the initial evaporation rate. To clarify this, we used FLEXPART to calculate the forward budget of *(E-P)i10* on air masses residing over C2 for May and August (Fig. 8), the two months when the extreme values of E-FLEX are the opposite of the local evaporation (E-GLEAM), as shown in Figure 7. In May, air masses forward-tracked from C2 lose moisture over C2 itself (blueish colours), and the moisture sinks are observed over the whole of the source and the northwest CRB, suggesting the influence of local recycling. This explains why E-FLEX is lower than E-GLEAM (Fig. 7). In August when E-FLEX is higher than E-GLEAM, on the south and west of C2 disappear as intense moisture sinks areas, and the air masses forward-tracked from C2 provide moisture to C2 itself over the north and east only (Fig. 8). This fact implies that recycling decreases and this could explain why E-FLEX is greater than local evaporation (E-GLEAM). On the other hand, it can be appreciated that moisture lost over the CRB during August from C2 is higher in the northwest of the basin and that the positive values of *(E-P)i0>0* are reduced in the south (Fig. 8), confirming that C2 is more effective in supplying moisture to the CRB during August.

To explain this relationship better, we also address the case for the CRB itself. For CRB the annual cycle of the E-GLEAM is characterized by maximum values during December-May and a minimum in July-August (Fig. 7, CRB). In January-February, April-October, and December, E-FLEX is higher than E-GLEAM, in accordance with the decreasing precipitation over the basin (Fig. 3). This is understandable because the moisture uptake E-FLEX over the basin itself must be favoured when the precipitation over it decreases. Comparing the precipitation annual cycle in the CRB (Fig. 3) with E-GLEAM (Fig. 7), it can

be seen that both show the same annual cycle, but they show opposite behaviour from E-FLEX (Fig. 7, CRB). This relationship describes a scheme in which the precipitation and evaporation are strongly lineally related and the moisture uptake is the opposite, determining when the source is more effective in providing moisture for itself. Moreover, this relationship is not strictly interdependent because it could be modulated by moisture income from the other sources.

Regarding the continental source of moisture, in the CRB the continental evaporation recycling efficiencies are high, and strong local recycling develops, or evaporative fluxes at least, and it is these that contribute to precipitation elsewhere on the continent throughout the year (van der Ent et al., 2014). The C3 source, separated from C2 by the Congo River mouth, follows a similar annual evaporation cycle to C2, but with lower values (<1 mm day^{-1}) during June-October (Fig. 7, C3). In addition, the E-FLEX values are higher than E-GLEAM in February and June-October. This indicates that during these months C3 is very efficient at providing moisture to the CRB. For the continental source C4, the annual cycle of local evaporation (E-GLEAM) is similar to C2, C3 and CRB, but the moisture uptake by air masses tracked backwards from the source (E-FLEX) to the CRB is always greater than E-GLEAM (unless in February), indicating that this source is very efficient in terms of moisture uptake for the CRB.

Located in the Arabian Sea, the O2 source shows two evaporation peaks during December-January and June, and two minima in April and September (Fig. 7). This cycle was also noted by Sadhuram and Kumar (1987), who showed that the maxima are related to strong winds, and the minima are a result of low wind speeds together with weak vapour pressure across the Arabian Sea. The moisture uptake over this source between April-October is almost insignificant, but the evaporation from OAFlux is greater, which means that this source is not efficient in delivering moisture to the CRB, because during these months it instead contributes to the Indian monsoon (Levine and Turner, 2012).

On the African continent, in C1 from May to October (boreal summer) E-GLEAM is higher than E-FLEX, and the opposite takes place in the other months, indicating when this source becomes more efficient in providing moisture to the CRB (Fig. 7, C1). The last source in the Atlantic (O3) has the smallest monthly average evaporation rate among all the oceanic sources throughout the year (<1 mm day^{-1}), showing a negligible annual cycle. Materia et al. (2012) determined that the evaporation rate from the ocean surface is lower due to the fact that part of this oceanic region is affected by the huge freshwater discharge of the Congo River, contributing to a decrease in Sea Surface Salinity (SSS) and Sea Surface Temperature (SST). Despite this, E-FLEX is greater than E-OAF except for during April and May, when the moisture uptake over this source is less than 1 mm day^{-1}. The moisture uptake has two peaks, one in February and the other in September-October.

3.4 Moisture contribution from the sources. Forward analysis.

Having identified the moisture sources regions, we determined the quantities and locations of the moisture loss over the CRB from those particles leaving each source using forward tracking. For this purpose, a forward experiment with FLEXPART was used, integrating particles forwards over 10 days. FLEXPART was used to compute the changes in *(E-P)* by tracking air parcels

regardless of whether it rains or not, but in this case we computed the result just for those particles arriving in the CRB that lost humidity.

Fig. 9 shows the monthly variation in the percentage of moisture contribution to the CRB with respect to the total income and the monthly mean precipitation over the CRB from CRU TS v.3.23 data (Harris et al., 2014). The basin itself turns out to be the most important moisture source throughout the year, contributing more than 55% each month (green line) to the total moisture supply from all the sources to the basin. The contribution from each of the remaining sources does not exceed 20% of the total. This result confirms the importance of moisture recycling over the basin, which differs from the result of van der Ent et al. (2010) who argued that the main source of rainfall in the Congo is moisture evaporating over East Africa, particularly over the Great Lake regions. This is probably a consequence of the method used; their approach takes account of how much of the evaporated water returns as precipitation to the same region (regional evaporation recycling), and what part of it is advected out of the region.

The annual cycle of the percentage moisture supply with respect to the total moisture contribution to the basin is quite similar for the C1 and C3 sources, at less than 4%. C2 and C4 are the most important continental sources (after the CRB itself) supplying moisture for the CRB across the year; they are located to the east and west, respectively, of the basin, and play opposite roles throughout the year. The moisture supply calculated from FLEXPART, $|(E-P)i10<0|$, for C4 follows the precipitation annual cycle in the basin particularly well. From the oceanic sources, the moisture contributions to the basin from O1 and O2 with respect to the total are less important than those from O3 and O4. It can be seen that the contribution from O3 increases and is thus important when the contribution decreases from the CRB itself, confirming the importance of moisture transport from the Atlantic Ocean. From the Indian Ocean, the contribution of moisture of O4 is at a maximum in January-February and July-August (>15%) when the precipitation rate decreases over the CRB (Fig. 3). The maximum monthly contribution from O4 occurs in April-May (~8%).

We analysed separately the percentage of moisture supplied from land-based and oceanic sources to the total moisture inflow to the CRB for the period 1980-2010. The results confirm that over the whole year the highest percentage (>50%) of the moisture contribution comes from the CRB itself (Fig. 10, green bars). The persistence of this result confirms the key importance of recycling in the basin. The atmospheric moisture supply to the CRB from the remaining land sources (red bars in Fig. 10) is higher than that provided by the oceanic sources (blue bars), apart from in August. In any case, the fact that the CRB is itself also a continental source means that the land regions are the most important in terms of atmospheric moisture contribution to the basin throughout the year.

The annual role of the moisture sources contributing to precipitation in the CRB is shown in Table 2 as the percentage of the total annual $|(E-P)i10<0|$ amounts over the CRB. The CRB itself is responsible for 59.3% and is the most effective source, followed by C4 with 12%, and O3 with 11.5%. These three sources together account for 82.8% of the total moisture supply to

the CRB in the climatological year. The remaining sources contribute 17.2% of the total precipitable moisture. The O1 source, located in the Red Sea, is responsible for just 0.2%.

Table 3 shows the results of a linear correlation analysis indicating the relationship between evaporation, precipitation, runoff, and river discharge series using the $|(E-P)i10<0|$ from each source over the CRB and the total $(E-P)i10<0$ from all the sources (T). All the correlation coefficients are positive and statistically significant at 95%, with the exception of that obtained between $|(E-P)i10<0|$ over the CRB from C2 and the Congo River discharge. The highest correlations were found for T, followed by the contribution supplied by the basin itself. In several cases, the correlation between the precipitation and the river discharge is reduced as a consequence of the lagged response of the hydrological system. In other cases, such as the correlation of |(E-P)i10<0| from O1 and C3 with runoff, the coefficient obtained is greater than that obtained with precipitation.

Fig. 11 shows the spatial relationship between the moisture supply from the sources and the precipitation over the CRB. The seasonal $|(E-P)i10<0|$ mean values over the CRB are plotted: December-February (DJF), March-May (MAM), June-August (JJA) and September-November (SON). Each map shows the correlation (shown bottom right) of these patterns with the respective climatological precipitation pattern over the basin (not shown).

The moisture sinks for the air masses transported from C1 to the CRB during DJF are more intense (~ -1.5 mm day^{-1}) on a belt located in the central-north part of the basin extending beyond it and to the south (Fig. 11). In MAM the maximum moisture loss moves northwards, and it almost disappears altogether in JJA, while for SON the moisture loss covers the entire CRB with major sinks located in the northern half, in agreement with the high rainfall observed during these months (see Fig. 2). For SON the best correlations were those between the patterns of $|(E-P)i10<0|$ from C1 and precipitation over the CRB (r=0.50). From C2, those sources located to the west of the CRB, the greatest moisture contribution occurs over the west of the basin. In MAM and JJA the $|(E-P)i10<0|$ patterns are observed over the northern half, and the best correlation was obtained for JJA (r=0.63). Contrary to what happens with moisture loss over the basin from C2, the greatest moisture sinks over the CRB for air masses tracked forwards from C3 are mostly positioned to the southwest (best observed for SON and DJF). In MAM and JJA, the sinks are mainly located in the northern half of the basin. From C4 (located to the east of the CRB) the sinks over the CRB decrease in intensity from east to west (the eastern areas show the most intense sinks, >6 mm day^{-1}). It is worth remembering that in southern equatorial Africa, and especifically in the CRB region, the precipitation pattern provides a mechanism of atmospheric communication between east and west Africa, these two equatorial regions being generally treated as climatically separate units (Dezfuli et al., 2015). As expected, during SON and DJF (rainiest months) the pattern of $|(E-P)i10<0|$ is more intense. The correlations vary between 0.36 and 0.43, all significant for $p<0.05$. Throughout the year the CRB is the most important moisture source for itself (Fig. 9 and 10), which is confirmed by the intensity of the values in the $|(E-P)i10<0|$ pattern (Fig. 11). In DJF and SON greatest moisture sinks (>12 mm day^{-1}) cover the major part of the centre and south of the basin. In MAM and JJA they are similar to the other sources. The correlation of these patterns with the spatial precipitation was the highest obtained ($r>0.63$).

We previously discussed how the oceanic source O1, despite being an important evaporative region, is not an effective moisture source for precipitation over the CRB. This fact can also be seen in the pattern of $|(E-P)i10<0|$ over the CRB in Fig. 11, where the values are low and oscillate around -0.5 to 0 mm day^{-1}. The pattern also reflects the north-south variability of the precipitation over the year. From the O2 source, located in the Arabian Sea, the greatest moisture contribution occurs in the east and northeast part of the basin, apart from in JJA when the pattern is confined to the northwest and the moisture loss is lower. The O3 source, in the east-tropical Atlantic Ocean, is the most important oceanic source for the CRB, as shown in Table 3. In DJF the major moisture sinks are over the southwest of the basin, in MAM and JJA the moisture loss is mainly over the central and north of the basin, and during SON it is over the east. These patterns show a good correlation with rainfall spatial distribution ($r>0.43$). From O4, located in the West Indian Ocean, the greatest moisture contribution during DJF occurs over the south, and along a longitudinal belt in the central of the basin in MAM; in JJA the major contribution can be detected over the northern part of the basin. During SON when the moisture loss from O4 covers practically the whole territory, with the highest loss over the east, the correlation with the precipitation pattern is negative, however ($r=-0.18$). The highest precipitation for these months is shows maxima over the north and west parts, which explains the negative correlation (Fig. 3).

A common characteristic of the $|(E-P)i10<0|$ patterns is that the most intense values are generally located near the moisture sources, as is clear for the contributions from C2, C3, O3, O4, and the CRB itself. The geographic location of the continental sources around the CRB and the dominant atmospheric circulation are the key factors that make this possible.

3.4 Moisture sources during severe dry and wet periods in the CRB.

We now consider the characteristics of the extreme hydrological conditions seen in the CRB. The temporal evolution of the 1- , 12- month SPEI series shows dry conditions during the periods: 1980-1985, 1992-1998 and 2004-2006, approximately (Fig. 12 a, b). The prevalence of wet conditions can be seen from 1985 to 1991 and from 2007 to 2010. Hydrological drought conditions at Kinsasha show temporal consistency with climate drought conditions (Fig. 12 c).

We calculated the monthly correlations between the anomalies of the total moisture influx to the basin $|(E-P)i10<0|$ (from all the sources together), runoff, and SSI for the 1- to 24- month SPEI time scales (Figure 13) in order to investigate any possible relationships. The significance of the correlation threshold was set at $p<0.05$. The correlation between $|(E-P)i10<0|$ monthly values and SPEI (Fig. 13a) shows significant and high values for all months, recorded for short SPEI time scales. Figure 13b shows the monthly correlation between the anomalies of runoff and SPEI. The relationship is positive and statistically significant from January to April within the 24 SPEI time scales, but it becomes negative when the precipitation decreases over the basin. Surface runoff seems to be strongly dependent on precipitation deficit for both shorter and annual rainfall deficit. When the rainfall increases over the basin from July to December, the correlation also increases. Correlations between SSI at Kinsasha and SPEI (1–24 months) show that the evolution of hydrological conditions is consistent with the meteorological rainfall deficit state over the basin (Figure 13c). In particular, the strongest and most significant correlations

were found with SPEI-5 to -7 during April; this suggests the most appropriate time scales to use when identifying the meteorological drought in terms of its relationship with streamflow in the Congo River.

To investigate separately the role of the moisture sources during drought and wet conditions in the CRB we selected a few years affected by severe and extreme conditions. For this purpose SPEI values at the 12-month time scale for December were used to diagnose the status of water balance throughout each year. Moreover, long drought time-scales are generally used to assess streamflow droughts (Svoboda et al., 2012). Besides, at this time scale it is appropriate to represent the water balance in a region where the precipitation climatology is dictated by latitudinal migration crossing the Equator over the year, such as occurs in the CRB.

During the period 1980-2010, the years 1995 and 1996 were characterized by severe (SPEI12_December = -1.69) and extreme (SPEI12_December= -2.06) drought conditions respectively, while 1982 is characterized as severely wet (SPEI12_December = 1.68). Fig. 14 shows the mean annual contribution from all sources and the anomaly of $|(E-P)i10<0|$ for each event. In 1982 the most important moisture contributions are from the basin itself (~120 mm day^{-1}), O3 (~28 mm day^{-1}), and C4 (~27 mm day^{-1}). The anomalies of $|(E-P)i10<0|$ from all the sources are positive, but they are particularly high for the basin itself (18 mm day^{-1}). In 1995 and 1996 the greatest moisture loss continues to be that from the air masses from the CRB itself, the oceanic source O3, and the continental C4. However, when the anomalies were analysed all the sources showed negative values, meaning that the moisture support was in fact less than the normal conditions seen in dry years. In 1995 the deficit in the contribution from the CRB and O4 is highlighted. Hua et al. (2016) described how an increase in subsidence across the western edge of Indian Ocean (O4) and a decrease in convection over the Congo Basin (CRB) led to a reduction in moisture transport and rainfall across Central Equatorial Africa. In 1996, a year characterized by extreme drought conditions, the negative anomaly in the moisture supply from all the sources remains, but that computed for the basin is higher than it was in 1995. Therefore, the moisture contribution for the CRB is essentially recycling for the three years considered, and constitutes a key element that modulates the conditions for droughts in the basin via the rainfall. To confirm these results, we calculated the spatial anomalies of the moisture losses for air masses tracked from the CRB (Fig. 15). In 1982 (a severe wet year) over the northern half of the basin high positive anomalies of $|(E-P)i10<0|$ values (> 3 mm day^{-1}) occur. For 1995, the anomalies are negative in the east and north of the basin, and cover almost the whole basin during the extremely dry year (1996).

4. Conclusions

The most important climatological moisture sources for the Congo River Basin have been identified using the Lagrangian model FLEXPART, for a 31-year dataset (1980-2010). To assess the relationship between these sources and the hydrological cycle in the basin the relationship with precipitation, runoff and river discharge in the basin were all assessed. The mean annual precipitation pattern in the CRB confirms the north-south dipole associated with the annual migration of the ITCZ. On average,

maximum rainfall occurs between October and April while minima are observed in June and July, always in good correlation with the runoff and Congo River discharge; in particular the monthly values of discharge have the best correlation (r=0.66) with precipitation having a lag of one month, which is the time taken for the runoff to be seen as freshwater in the Congo River. The backward tracking of air masses reveals that the CRB receives humidity from both hemispheres. At an annual scale, four oceanic sources were identified in the Atlantic Ocean, the Indian Ocean and the Red Sea, while the continent contains four sources surrounding the CRB, as well as the basin itself, which acts as its own moisture source. The importance of each source in the moisture uptake of the CRB confirms the main role of the CRB on the negative budgets of (E-P) over the basin itself, representing more than 50% of the total moisture loss over the basin supplied by all sources. Hence local recycling processes are hugely important, as pointed out by other authors. Other important sources providing moisture to the CRB are the tropical Atlantic Ocean (O3) and the continental region in the east of the target area (C4). At the same time, the source O1 located on the Red Sea, despite its high evaporation rate, is considered the least efficient source for providing humidity to the basin. Not only does the efficiency of the sources providing moisture to the CRB depend on the evaporation rate, it also influences the amount of water vapour transported to the basin, making the sources more or less effective in terms of precipitation over the CRB. Indeed, the spatial variability of the patterns of $(E\text{-}P)i10<0$ over the CRB after tracking the air masses forwards from all the sources confirms the link between the geographical location of the sources and the location of the greatest moisture sinks over the basin, associated with atmospheric circulation. These patterns show a good correlation with precipitation over the basin and demonstrates the ability of FLEXPART to reproduce the temporal and spatial variability of the precipitation over the CRB. The roles of the sources providing moisture during years with extreme and severe conditions confirm the key role of the CRB in modulating the water balance within itself.

Moreover, it has clearly been shown that dry (wet) periods in the basin are clearly connected with positive (negative) anomalies of P-E in the CRB, mainly in the northern part of the basin. This suggests that during both dry and wet periods, recycling over the basin is of primary importance.

The complex nature of the hydrological feedback mechanisms in the Congo River Basin is now better understood thanks to the identification of the continental and oceanic moisture sources. The results obtained will also support further studies to address the role of these moisture sources during climate extremes such as flooding, droughts, and extreme discharge events in the Congo River, among others. One important aspect for consideration in future research is related to the possible influence of Modes of Climate Variability (such as ENSO, SOI, or QBO) on the modulation of moisture transport from these sources to the CRB.

Acknowledgements. This work was supported by EPhysLab (UVIGO-CSIC Associated Unit). R. Sorí would like to acknowledge the grant received by the Xunta of Galicia, Spain, in support of his doctoral research work; R. Nieto acknowledges the support provided by CNPq grant 314734/2014-7 from the Brazilian government, and A. Drumond

acknowledges the support of the Spanish Government and FEDER via 437, the SETH (CGL2014-60849-JIN) project and IMDROFLOOD financed by the Water Works 2014 co-funded call of the European Commission.

References

Abdulaziz, S.: Annual and Seasonal Mean Net Evaporation Rates of the Red Sea Water during Jan 1958 – Dec 2007. MSc. thesis, University of Bergen, 2012.

Alemaw, B. F.: Hydrological Modeling of Large Drainage Basins Using a GIS-Based Hybrid Atmospheric and Terrestrial Water Balance (HATWAB) Model. J. of Water Resource and Protection., 4, 516-522, 2012.

Alsdorf, D., Beighley, E., Laraque, Alain., Lee, H., Tshimanga, R., O'Loughlin, F., Mahé, G., Dinga, B., Moukandi, G., and Spencer, R. G. M.: Opportunities for hydrologic research in the Congo Basin. Rev. Geophys., 54, doi:10.1002/2016RG000517, 2016.

Bates, B. C., Kundzewicz, Z.W., Wu, S., and J. P. Palutikof.: Climate Change and Water. Technical Paper of the Intergovernmental Panel on Climate Change, IPCC Secretariat, Geneva, 210 pp., 2008.

Camberlin, P., Janicot, S., and Poccard, I.: Seasonality and atmospheric dynamics of the teleconnection between african rainfall and tropical sea-surface temperature: Atlantic vs. Enso, Int. J. Climatol., 21: 973–1005 (2001). doi: 10.1002/joc.673, 2001.

Castillo, R., Nieto, R., Drumond, A., Gimeno, L.: Estimating the Temporal Domain when the Discount of the Net Evaporation Term Affects the Resulting Net Precipitation Pattern in the Moisture Budget Using a 3-D Lagrangian Approach, PLoS ONE., 9(6): e99046. doi:10.1371/journal.pone.0099046, 2014.

Chao,Yi., Farrara, J. D., Schumann, Guy., Andreadis, K. M., Moller, D.: Sea surface salinity variability in response to the Congo river Discharge, Continental Shelf Research., 35–45, 2015.

Chen, B., Xu, X. D., Yang, S., and Zhang, W.: Theor Appl Climatol., 110: 423. doi:10.1007/s00704-012-0641-y, 2012.

Chishugi, J. B.: Hydrological modelling of the congo river basin: a soil-water balance approach. MSc. thesis, University of Botswana, 2008.

Dai, A.: Increasing drought under global warming in observations and models. Nature Climate Change. 3: 52-58, 2013.

Dai, A., and Trenberth, K. E.: Estimates of Freshwater Discharge from Continents: Latitudinal and Seasonal Variations, J. of Hidrometeorolgy., 3, 660-687, 2002.

Dai, A., Qian, T., and Trenberth, K. E.: Changes in Continental Freshwater Discharge from 1948-2004, J. Climate., 2773-2792, doi: 10.1175/2008JCLI2592.1, 2008.

Dirmeyer, P. A., and Brubaker, K. L.: Contrasting evaporative moisture sources during the drought of 1988 and the flood of 1993, J. Geophys. Res., 104, 383–19,397, doi:10.1029/1999JD900222, 1999.

Dirmeyer, P. A., Brubaker, K. L., and DelSole, T.: Import and export of atmospheric water vapor between nations, J. Hydrol., 365, 11–22, doi:10.1016/j.jhydrol.2008.11.016, 2009.

Drumond, A., Marengo, J., Ambrizzi, T., Nieto, R., Moreira, L., and Gimeno, L.: The role of the Amazon Basin moisture in the atmospheric branch of the hydrological cycle: a Lagrangian analysis, Hydrol. Earth Syst. Sci., 18, 2577–2598, doi:10.5194/hess-18-2577-2014, 2014.

Druyan, L. M., Koster, R. D.: Sources of Sahel Precipitation for Simulated Drought and Rainy Seasons, J. Clim., 2, 1438–1446, 1989.

Dee, D. P., and 35 co-authors.: The ERA-Interim reanalysis: Configuration and performance of the data assimilation system, Quart. J. R. Meteorol. Soc.. 137, 553-597, doi: 10.1002/qj.828, 2011.

Dezfuli, A. K., Zaitchik, B. F., and Gnanadesikan, A.: Regional Atmospheric Circulation and Rainfall Variability in South Equatorial Africa, J. of Climate., 28, 809-818, doi:10.1175/JCLI-D-14-00333.1, 2015.

Drumond, A., Marengo, J., Ambrizzi, T., Nieto, R., Moreira, L., Gimeno, L.: The role of the Amazon Basin moisture in the atmospheric branch of the hydrological cycle: A Lagrangian analysis, Hydrol. Earth Syst. Sci., 18, 2577–2598, doi:10.5194/hess-18-2577-2014, 2014.

Drumond, A., Nieto, R., Gimeno, L.: A Lagrangian approach for investigating anomalies in the moisture transport during drought episodes, Cuadernos de Investigación Geográfica., 42, 113-125, doi: 10.18172/cig.2925, 2016a.

Drumond, Anita.; Taboada, E.; Nieto, R.; Gimeno, L.; Vicente-Serrano, S. M.; López-Moreno, J. I. A Lagrangian analysis of the present-day sources of moisture for major ice-core sites. Earth Syst. Dynam. 2016, 7, 549–558, doi:10.5194/esd-7-549-2016, 2016b.

Druyan, L. M., and Koster, R. D.: Sources of Sahel Precipitation for Simulated Drought and Rainy Seasons, J. of Climate., 2, 1438-1446, 1989.

Eltahir, E. A. B., and Bras, R. L.: Precipitation recycling, Rev. Geophys., 34, 367–378, doi:10.1029/96RG01927, 1996.

Eltahir, E. A. B., and Gong, C.: Dynamics of Wet and Dry years in West Africa, J. of Climate., 9, 1030-1042, doi:10.1175/1520-0442, 1996.

Gimeno, L.: Grand challenges in atmospheric science. Front. Earth Sci. 1:1. doi: 10.3389/feart.2013.00001, 2013a.

Gimeno, L., Drumond, A., Nieto, R., Trigo, R. M., and Stohl, A.: On the origin of continental precipitation, Geophysical Research Letters., 37, L13804, doi:10.1029/2010GL043712, 2010.

Gimeno, L., Stohl, A., Trigo, R. M., Dominguez, F., Yoshimura, K., Yu, L., and et al.: Oceanic and terrestrial sources of continental precipitation. Rev. Geophys. 50, RG4003. doi: 10.1029/2012RG000389, 2012.

Gimeno, L., Nieto, R., Drumond, A., Castillo, R., and Trigo, R.: Influence of the intensification of the major oceanic moisture sources on continental precipitation, Geophys. Res. Lett., 40, doi:10.1002/grl.50338, 2013b.

Harris, I., Jones, P. D., Osborn, T. J. and Lister, D. H.: Updated high-resolution grids of monthly climatic observations – the CRU TS3.10 Dataset, Int. J. Climatol., 34, 623–642. doi:10.1002/joc.3711, 2014.

Hua, W., Zhou, L., Chen, H., Nicholson, S. E., Raghavendra, A., and Jiang, Y.: Possible causes of the Central Equatorial African long-term drought, Environ. Res. Lett., 11, 1-13, 2016.

Hugues, NLOM. J.: The Economic Value of Congo Basin Protected Areas Goods and Services, J. of Sustainable Development., Vol. 4, No. 1, 130-142, 2011.

Haensler, A., Saeed, F. and Jacob, D.: Assessment of projected climate change signals over central Africa based on a multitude of global and regional climate projections, in: Climate Change Scenarios for the Congo Basin. Climate Service Centre Report No. 11, Hamburg, Germany, ISSN: 2192-4058, 2013.

International Bussines Publications (IBP).: Congo, Land Ownership and Agricultural Laws Handbook. Volume 1, Strategic Information and Regulation. Edition Updated Reprint International Business Publications, Washington, USA, 2015.

Intergubernamental Pannel of Climate Change (IPCC).: Cambio climático 2007: Informe de síntesis. Contribución de los Grupos de trabajo I, II y III al Cuarto Informe de evaluación del Grupo Intergubernamental de Expertos sobre el Cambio Climático, IPCC, Ginebra, Suiza, 2007.

Jackson, B., Nicholson, S. E., and Klotter, D.: Mesoscale convective systems over western equatorial Africa and their relationship to largescale circulation, Mon. Weather Rev., 137, 1272–1294, doi:10.1175/2008MWR2525.1, 2009.

Lee, H., Edward, R. B., Alsdorf, D., Jung H. C., Shum, C. K., Duan, J., Guo, J., Yamazaki, D., and Andreadis, K.: Characterization of terrestrial water dynamics in the Congo Basin using GRACE and satellite radar altimetry, Remote Sensing of Env., 115, 3530–3538, doi:10.1016/j.rse.2011.08.015, 2011.

Lehner, B., and Grill, G.: Global river hydrography and network routing: baseline data and new approaches to study the world's large river systems. Hydrological Processes., 27, 15, 2171–2186, 2013.

Levine, R. C. and Turner, A. G.: Dependence of Indian monsoon rainfall on moisture fluxes across the Arabian Sea and the impact of coupled model sea surface temperature biases, Climate Dyn., 38, 11-12, pp. 2167-2190, ISSN 0930-7575, 2012.

Lobell, D.B., Bänziger, M., Magorokosho, C., Vivek, B.: Nonlinear heat effects on African maize as evidenced by historical yield trials, Nature Climate Change., 1 (1), 42-45, 2011a.

Lobell, D.B., Schlenker, W., Costa-Roberts, J.: Climate trends and global crop production since 1980, Science., 333 (6042), 616-620, 2011b.

Marengo, J. A.: The characteristics and variability of the atmospheric water balance in the Amazon basin: Spatial and temporal variability, Climate Dyn., 24, 11-22, 2005.

Masih, I., Maskey, S., Mussá, F. E. F., and Trambauer, P.: A review of droughts on the African continent: a geospatial and long-term perspective, Hydrol. Earth Syst. Sci., 18, 3635–3649, doi:10.5194/hess-18-3635-2014, 1014.

Materia, S., Gualdi, S., Navarra, A., and Terray, L.: The effect of Congo River freshwater discharge on Eastern Equatorial Atlantic climate variability, Climate Dyn., 39, 2109–2125, doi:10.1007/s00382-012-1514-x, 2012.

Nieto, R., Gimeno, L., and Trigo, R. M.: A Lagrangian identification of major sources of Sahel moisture, Geophys. Res. Lett., 33, L18707, doi:10.1029/2006GL027232, 2006.

Nicholson, S. E., and Grist, J. P.: The seasonal evolution of the atmospheric circulation over West Africa and Equatorial Africa, J. Clim., 16, 7, 1013–1030, 2003.

Nieto, R., Gallego, D., Trigo, R. M., Ribera, P., and Gimeno, L.: Dynamic identification of moisture sources in the Orinoco basin in equatorial South America, Hydrol. Sci. J., 53, 602–617, 2008.

Numaguti, A.: Origin and recycling processes of precipitating water over the Eurasian continent: Experiments using an atmospheric general circulation model, J. Geophys. Res., 104, 1957–1972, 1999.

Owiti, Z., and Zhu, W.: Spatial distribution of rainfall seasonality over East Africa, J. of Geography and Regional Planning., 5 (15), 409-421, doi:10.5897/JGRP12.027, 2012.

Peixoto, J.P., and Oort, A.H. (1992) Physics of climate. Springer, Berlin.

Peixoto, J. P., and Oort, A. H.: Physics of Climate. AIP-Press, New York, NY: Springer–Verlag New York Press, 1992.

Pokam, W. M., Djiotang, L. A. T., and Mkankam, F. K.: Atmospheric water vapor transport and recycling in Equatorial Central Africa through NCEP/NCAR reanalysis data, Climate Dyn., 38, 1715–1729, doi:10.1007/s00382-011-1242-7, 2012.

Rwetabula, J., De Smedt, F., and Rebhun, M.: Prediction of runoff and discharge in the Simiyu River (tributary of Lake Victoria, Tanzania) using the WetSpa model, Hydrol. Earth Syst. Sci. Discuss., 4, 881-908, 2007.

Salih, A. A. M., Zhang, Q., and Tjernström, M.: Lagrangian tracing of Sahelian Sudan moisture sources, J. Geophys. Res. Atmos., 120, 6793–6808, doi:10.1002/2015JD023238, 2015.

Samba, G., and Nganga, D.: Rainfall variability in Congo-Brazzaville: 1932–2007, Int. J. Climatol., 32: 854-873, doi:10.1002/joc.2311, 2012.

Secretariat of the Convention on Biological Diversity and Central African Forests Commission (SCBD-CAFC).: Biodiversity and Forest Management in the Congo Basin, Montreal, 2009.

Siam, M. S., Marie-Estelle, D., and Elfatih A. B. E.: Hydrological Cycles over the Congo and Upper Blue Nile Basins: Evaluation of General Circulation Model Simulations and Reanalysis Products, J. Climate., 26, 22, 8881–8894, 2013.

Sodemann, H., Schwierz, C., and Wernli, H.: Interannual variability of Greenland winter precipitation sources: Lagrangian moisture diagnostic and North Atlantic Oscillation influence, J. Geophys. Res., 113, D03107, doi:10.1029/2007JD008503, 2008.

Sofianos, S. S., Johns, W. E., and Murray, S. P.: Heat and freshwater budgets in the Red Sea from direct observations at Bab el Mandeb. Deep Sea Research Part II: Topical Studies in Oceanography, 49 (7-8):1323–1340, 2002.

Stohl, A., and James, P.: A Lagrangian analysis of the atmospheric branch of the global water cycle. Part I: Method description, validation, and demonstration for the August 2002 flooding in central Europe, J. Hydrometeorol., 5, 656–678, doi:10.1175/1525-7541(2004)005<0656: ALAOTA>2.0.CO;2, 2004.

Stohl, A., and James, P.: A Lagrangian analysis of the atmospheric branch of the global water cycle. Part II: Moisture transports between the Earth's ocean basins and river catchments, J. Hydrometeorol., 6, 961–984, doi:10.1175/JHM470.1, 2005.

Suzuki, T.: Seasonal variation of the ITCZ and its characteristics over central Africa, Theor Appl Climatol., 103:39–60, doi: 10.1007/s00704-010-0276-9, 2011.

Tan, Ch., Yang, J., and Li, Man.: Temporal-Spatial Variation of Drought Indicated by SPI and SPEI in Ningxia Hui Autonomous Region, China, Atmosphere., 6, 1399-1421, doi:10.3390/atmos6101399, 2015.

The Center for Ocean-Land-Atmosphere Studies: http://cola.gmu.edu/wcr/river/, last access 02 February 2017.

Trenberth, K. E.: Atmospheric Moisture Recycling: Role of Advection and Local Evaporation, J. of Climate., 12, 1368-1380, 1999.

van der Ent, R. J., Savenije, H. H. G., Schaefli, B., and Steele-Dunne, S. C.: Origin and fate of atmospheric moisture over continents, Water Resour. Res., 46, 1-12, doi:10.1029/2010WR009127, 2010.

van der Ent, R. J., Wang-Erlandsson, L., Keys, P. W., and Savenije, H. H. G.: Contrasting roles of interception and transpiration in the hydrological cycle – Part 2: Moisture recycling. Earth Syst. Dynam., 5, 471–489, doi:10.5194/esd-5-471-2014, 2014.

Vicente-Serrano, S.M., Beguería, S., López-Moreno, J. I.: A Multiscalar Drought Index Sensitive to Global Warming: The Standardized Precipitation Evapotranspiration Index, J. of Climate., 23, 1696-1718, doi: 10.1175/2009JCLI2909.1, 2010.

Vicente-Serrano, S. M., López-Moreno, J. I., Santiago, B., Lorenzo-Lacruz, J., Azorin-Molina, C., and Morán-Tejeda, E.: Accurate computation of a streamflow drought index., J. of Hyd. Eng., 17: 318-332, 2012.

Viste, E., and Sorteberg, A.: The effect of moisture transport variability on Ethiopian summer precipitation, Int. J. Climatol., 33: 3106–3123, doi:10.1002/joc.3566, 2013.

Wang, Q., Wu, J., Lei, T., He, B., Wu, Z., Liu, M., Mo, X., Geng, G., Li, X., Zhou, H., and Liu, D.: Temporal-spatial characteristics of severe drought events and their impact on agriculture on a global scale, *Quat. Int.*, 349, 10–21, 2014.

Washington, R., James, R., Pearce, H., Pokam, W. M., Moufouma-Okia, W.: Congo Basin rainfall climatology: can we believe the climate models?, Phil. Trans. R. Soc. B., 368, 20120296, doi:10.1098/rstb.2012.0296, 2013.

Svoboda, M., Hayes, M., and Wood, D.: Standardized Precipitation Index User Guide, World Meteorological Organization (WMO-No. 1090), Geneva, 2012.

Li, F., and Ramanathan, V.: Winter to summer monsoon variation of aerosol optical depth over the tropical Indian Ocean. J. of Geoph. Res., 107, 4284, doi:10.1029/2001JD000949, 2002.

Yu, L.: Global Variations in Oceanic Evaporation (1958–2005): The Role of the Changing Wind Speed, J. of Climate., 20, 5376-5390, doi: 10.1175/2007JCLI1714.1, 2007.

Zhou, L., Tian , Y., Myneni, R. B., Ciais, P., Saatchi, S., Liu, Y. Y., Piao, Shilong., Chen, H., Vermote, E. F., Song, C., Hwang, T.: Widespread decline of Congo rainforest greenness in the past decade, Nature., 86, VOL:509, doi:10.1038/nature13265, 2014.

Table 1. Mean annual Evaporation rate over the sources. Data for the continent were obtained from GLEAM and for the ocean from OAflux.

	Evaporation rate (mm day^{-1})								
Sources	C1	C2	C3	C4	CRB	O1	O2	O3	O4
	1.0	2.5	1.6	1.5	2.4	4.6	1.1	0.71	4.7

Table 2. Moisture contribution from the sources to the CRB (%).

(E-P)i10<0 in %

Earth Syst. Dynam. Discuss., doi:10.5194/esd-2017-21, 2017
Manuscript under review for journal Earth Syst. Dynam.
Discussion started: 9 March 2017

Earth System Dynamics Discussions Open Access EGU

Sources	C1	C2	C3	C4	CRB	O1	O2	O3	O4
	2.3	6.8	2.1	**12.0**	**59.3**	0.2	1.8	**11.5**	4.1

Table 3. Significant monthly correlation ($p<0.05$) between the precipitation from CRU, Runoff from ERA-Int, River discharge from the GRDC and evaporation from GLEAM or OAFLUX, and series of $|(E-P)i10<0|$ forward-integrated using FLEXPART from the sources over the CRB, and with the total $|(E-P)i10<0|$ amount (T). Period used: 1980 – 2010.

	C1	**C2**	**C3**	**C4**	**CRB**	**O1**	**O2**	**O3**	**O4**	**T**
Evaporation	0.35		0.35	0.36	0.37	0.35	0.43	0.14	0.35	0.36
Precipitation	0.60	0.53	0.65	0.77	0.80	0.36	0.58	0.60	0.58	0.83
Runoff	0.66	0.43	0.72	0.69	0.75	0.59	0.73	0.59	0.43	0.75
Discharge	0.49		0.59	0.53	0.54	0.47	0.55	0.33	0.12	0.53

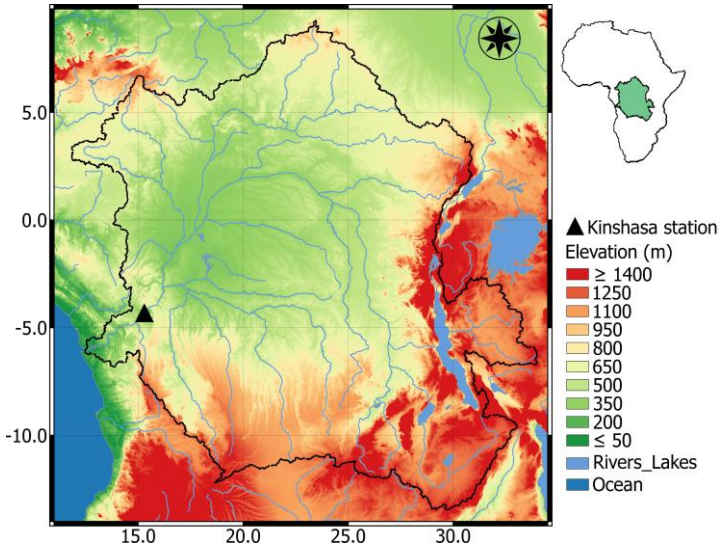

Figure 1. Geographic location of the Congo River Basin showing the Kinshasa gauging station, the fluvial system and elevations (source: Hydrosheds project).

Earth Syst. Dynam. Discuss., doi:10.5194/esd-2017-21, 2017
Manuscript under review for journal Earth Syst. Dynam.
Discussion started: 9 March 2017

Earth System Dynamics
Discussions
Open Access
EGU

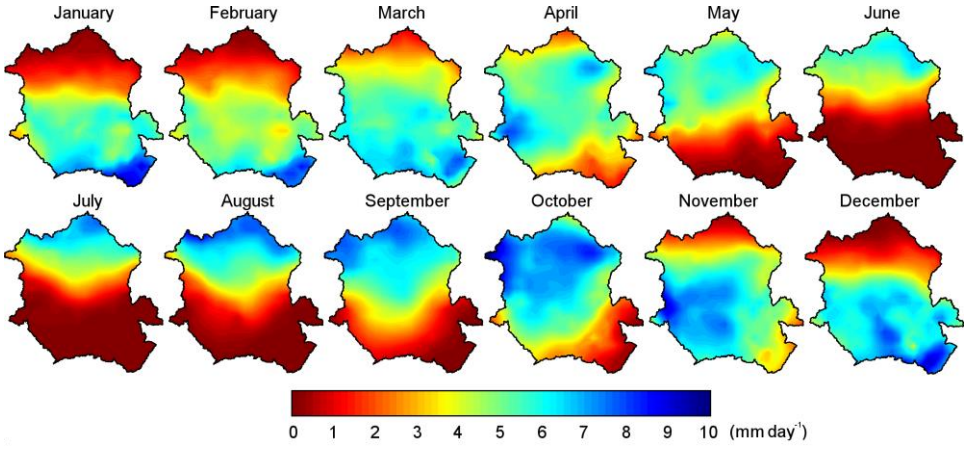

Figure 2. Monthly mean precipitation over the CRB for 1980-2010. Data from CRU TS v.3.23.

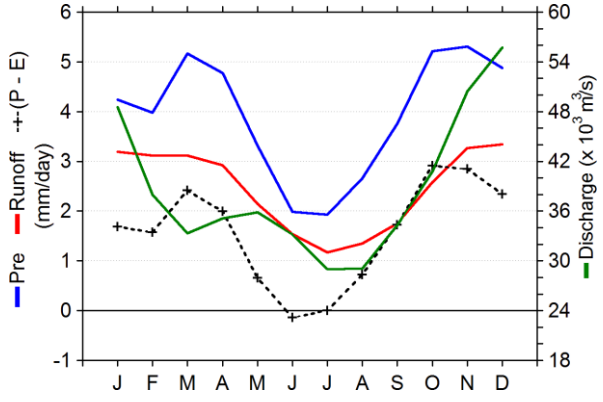

Figure 3. Annual cycle of precipitation, runoff and (P-E) in the CRB (left axis), and the Congo River discharge (right axis). Data obtained from CRU, ERA-Int, GLEAM and Global Runoff Data Center, respectively.

Earth Syst. Dynam. Discuss., doi:10.5194/esd-2017-21, 2017
Manuscript under review for journal Earth Syst. Dynam.
Discussion started: 9 March 2017

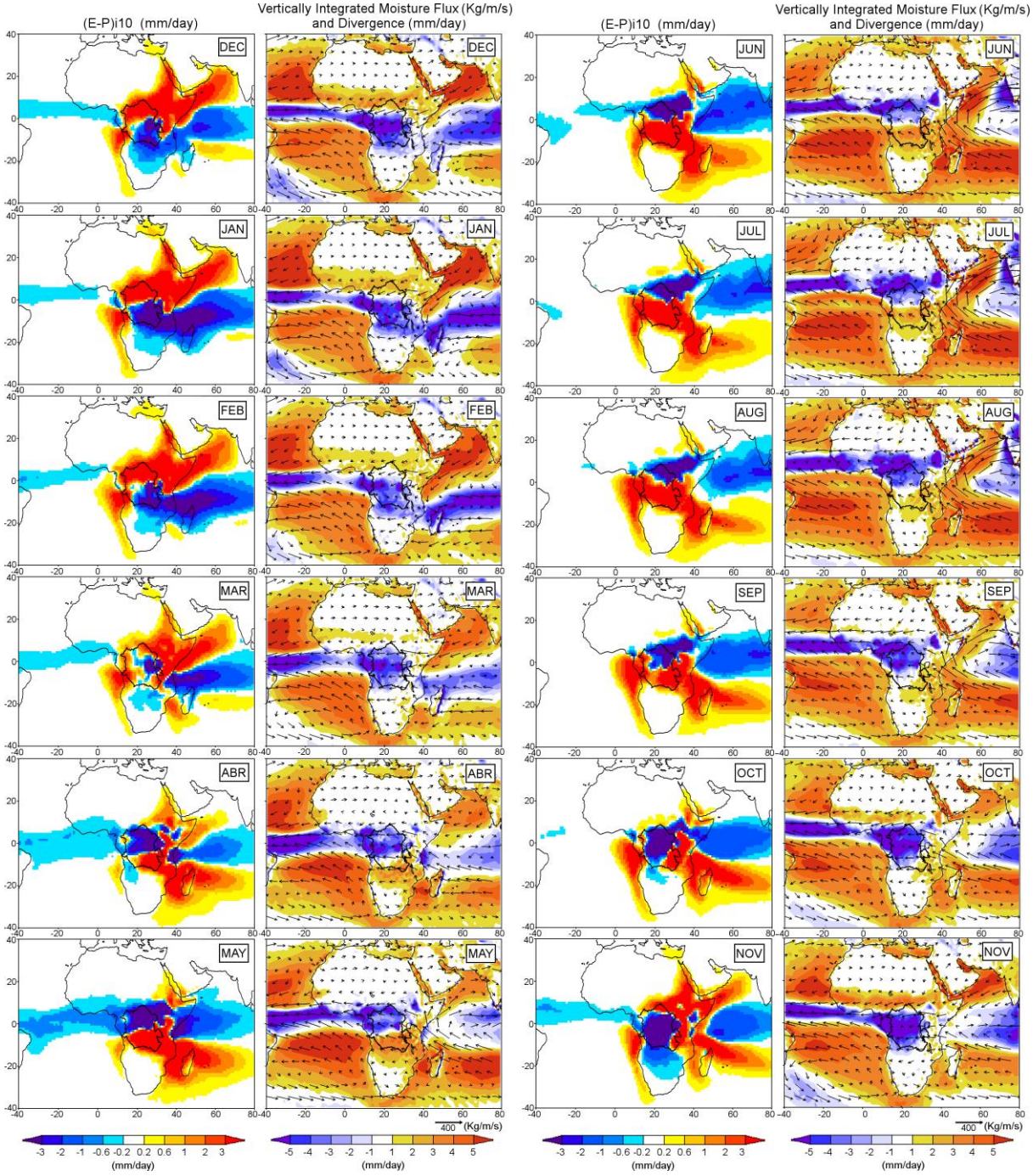

Figure 4. Monthly climatological (E-P) values integrated backwards over 10 days (mm day^{-1}) alongside Vertically Integrated Moisture Flux (kg/m/s) and divergence-convergence (reddish-blueish colours) (mm day^{-1}). Period 1980 - 2010.

Earth Syst. Dynam. Discuss., doi:10.5194/esd-2017-21, 2017
Manuscript under review for journal Earth Syst. Dynam.
Discussion started: 9 March 2017

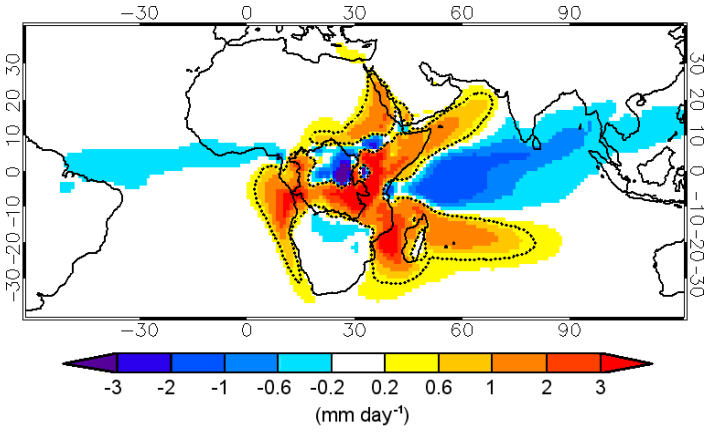

Figure 5. Annual mean values of *(E-P)i10* backward-integrated over 10 days for the period 1980-2010. Dashed lines represent the boundaries of the sources of moisture, defined as p90= 0.4 mm day^{-1}.

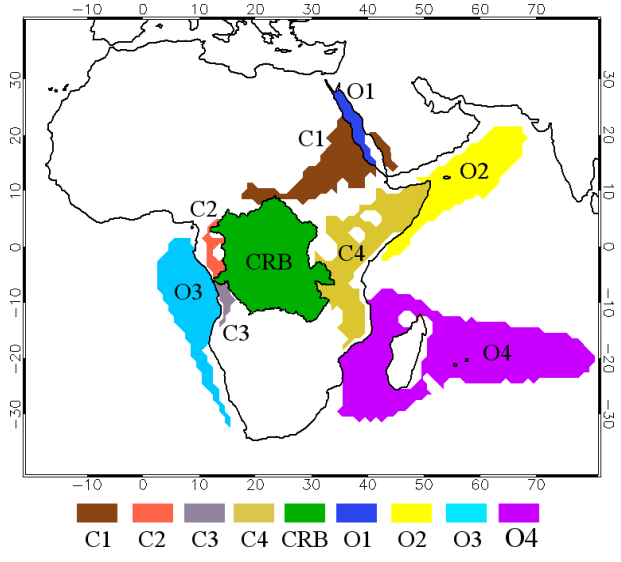

Figure 6. Continental moisture sources for CRB: C1, C2, C3, C4, and the CRB itself; Oceanic moisture sources: O1, O2, O3, and O4.

Earth Syst. Dynam. Discuss., doi:10.5194/esd-2017-21, 2017
Manuscript under review for journal Earth Syst. Dynam.
Discussion started: 9 March 2017

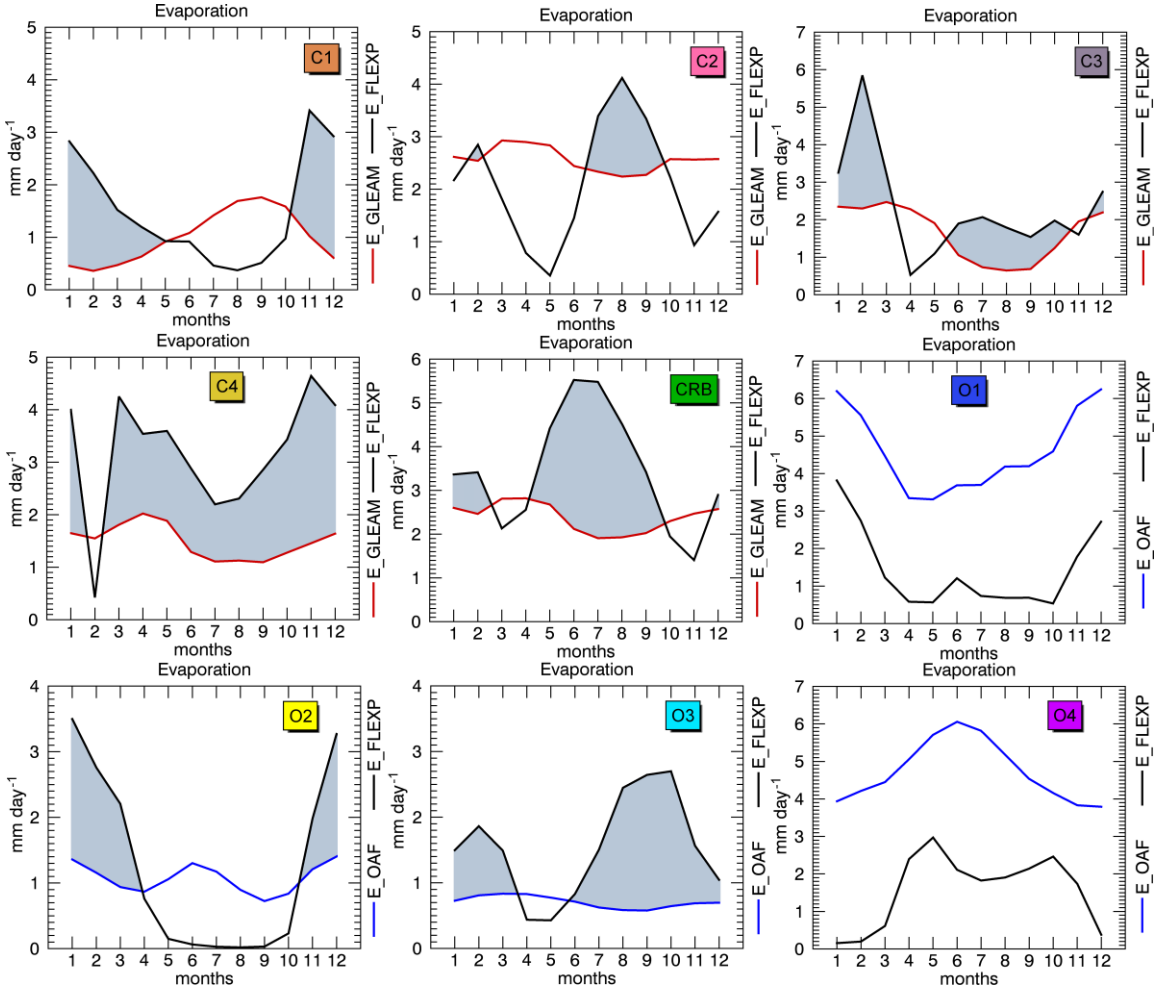

Figure 7. Monthly mean evaporation in continental (C) and oceanic (O) sources (in mm day^{-1}). Data from GLEAM (red lines) and OAFlux (blue lines). E-FLEX: evaporation values over the sources obtained using FLEXPART (black lines). Areas shaded in gray identify where E-FLEX > Evaporation. Data period: 1980-2010.

Earth Syst. Dynam. Discuss., doi:10.5194/esd-2017-21, 2017
Manuscript under review for journal Earth Syst. Dynam.
Discussion started: 9 March 2017

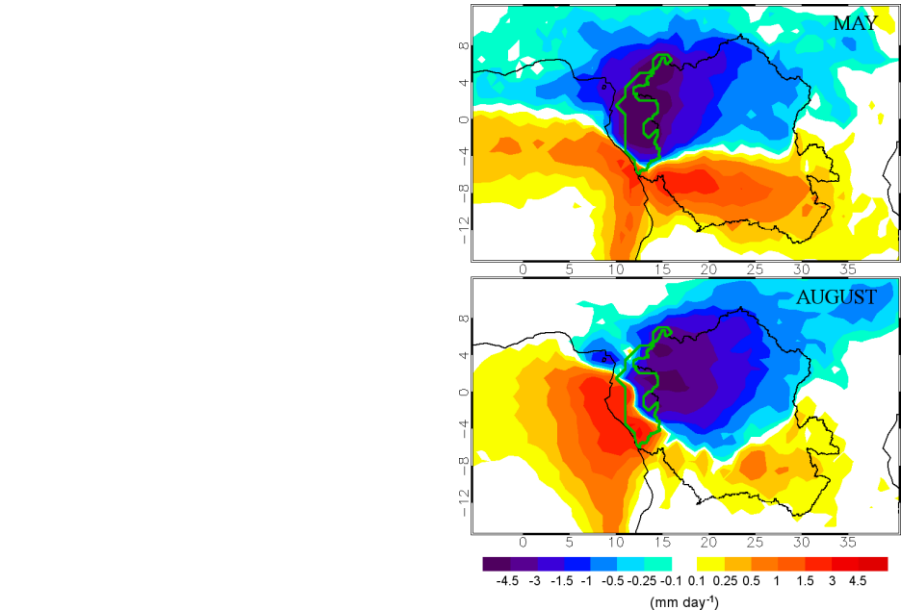

Figure 8. Forward *(E-P)*i10 from the moisture source C2 (green contour line) for May (top) and August (bottom). Period 1980-2010.

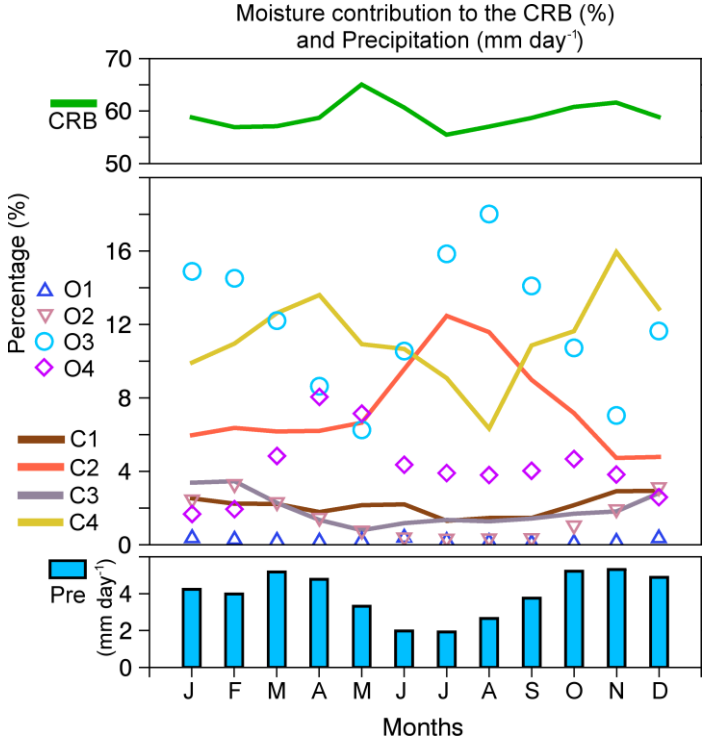

Earth Syst. Dynam. Discuss., doi:10.5194/esd-2017-21, 2017
Manuscript under review for journal Earth Syst. Dynam.
Discussion started: 9 March 2017

Figure 9. Monthly percent of moisture loss calculated as |(E-P)i10<0| forward-integrated from each source over the CRB over 10 days of transport, and monthly mean precipitation from CRU datasets for the period 1980-2010.

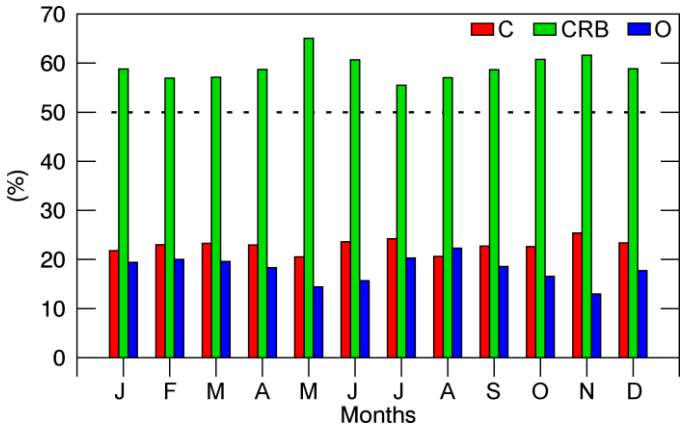

Figure 10. Monthly percentage moisture contributions to the CRB from continental sources (red bars), the CRB itself (green bars), and oceanic sources (blue bars). Data from FLEXPART for the period 1980-2010.

Earth Syst. Dynam. Discuss., doi:10.5194/esd-2017-21, 2017
Manuscript under review for journal Earth Syst. Dynam.
Discussion started: 9 March 2017

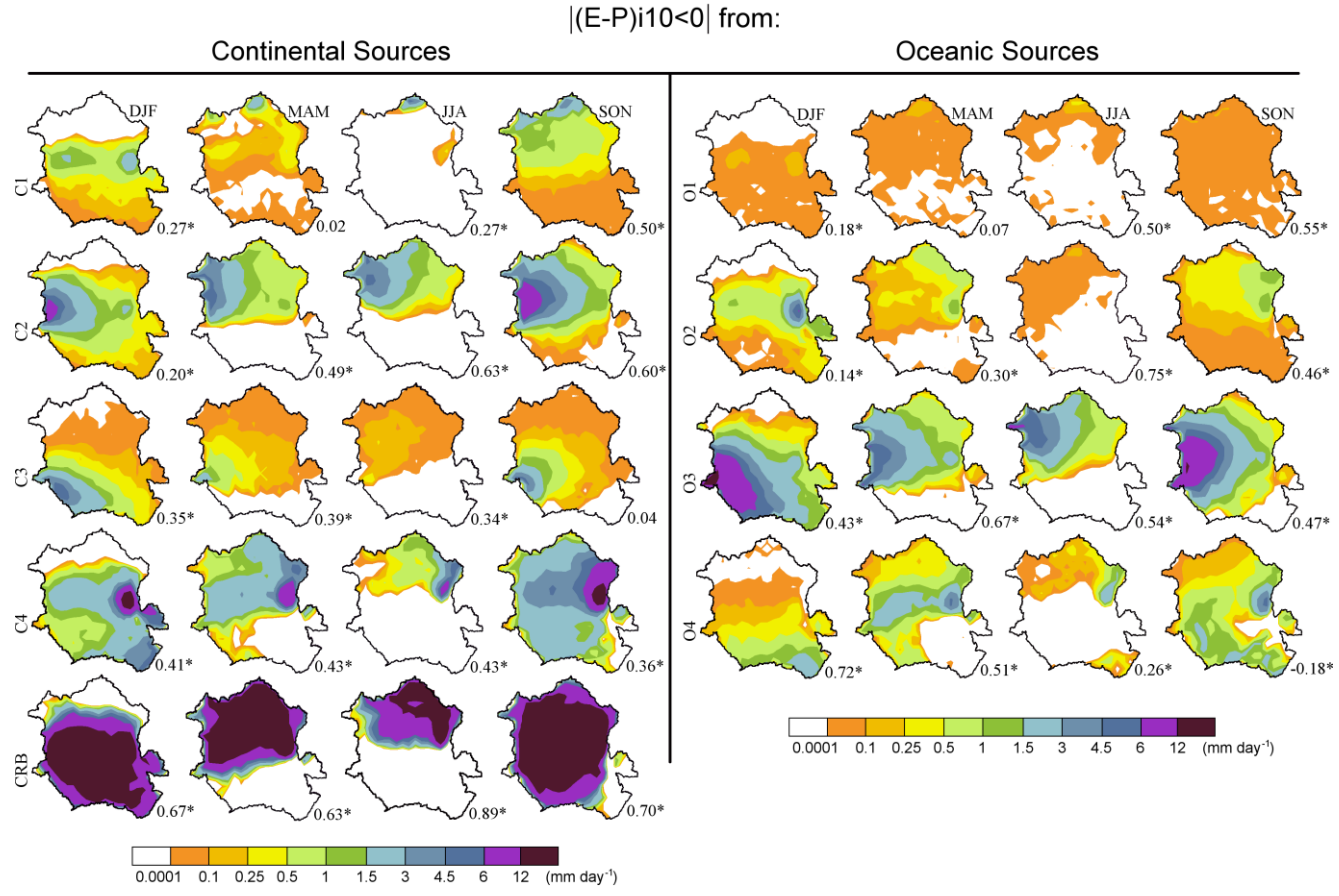

Figure 11. Seasonal mean *|(E-P)i10<0|* integrated forwards from the moisture sources over the CRB, in mm day^{-1}. The number in the bottom-right corner of each plot indicates the correlation with the mean precipitation pattern (asterisks indicate significant values at p<0.05). Period 1980- 2010.

Earth Syst. Dynam. Discuss., doi:10.5194/esd-2017-21, 2017
Manuscript under review for journal Earth Syst. Dynam.
Discussion started: 9 March 2017

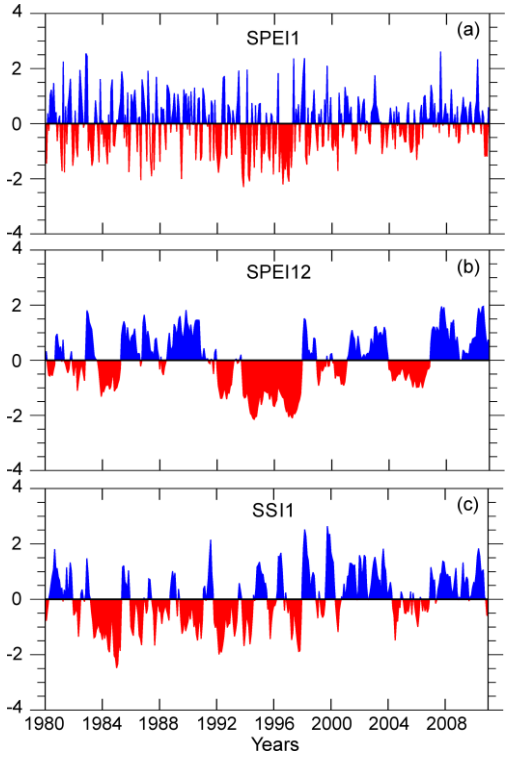

Figure 12. Time evolution of the SPEI in the Congo River basin at 1 (a), and 12 months (b) and Standardized Streamflow Index (SSI) (c) computed for the Congo River discharge. Period 1980 – 2010.

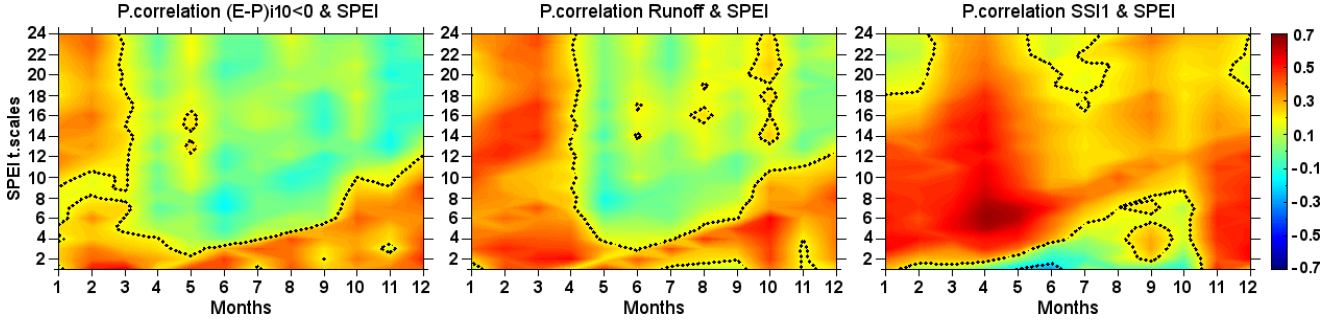

Figure 13. Monthly correlations between $|(E-P)i10<0|$, runoff and SSI with SPEI-1 to SPEI-24 in the Congo River Basin. Dotted lines represent significant correlations at $p<0.05$.

Earth Syst. Dynam. Discuss., doi:10.5194/esd-2017-21, 2017
Manuscript under review for journal Earth Syst. Dynam.
Discussion started: 9 March 2017

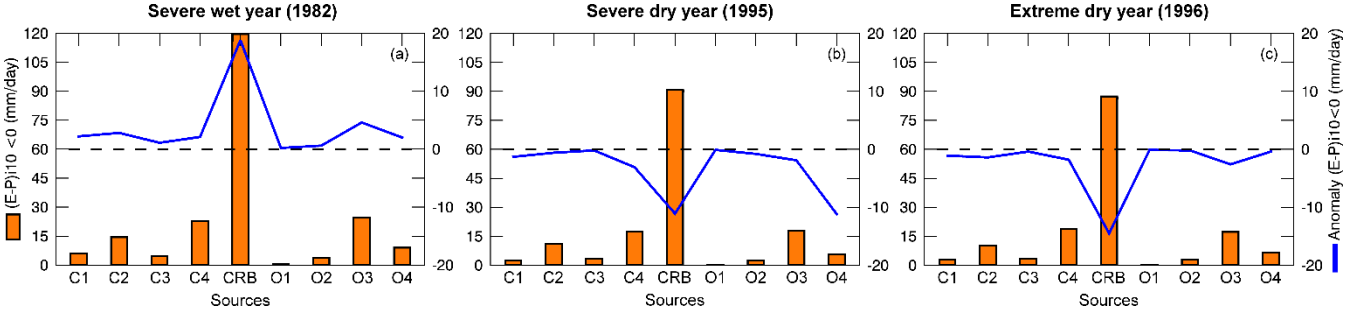

Figure 14. Mean annual moisture contribution from the sources to the CRB (orange bars) during 1982 (severe wet conditions, a), 1995 (severe dry conditions, b) and 1996 (extreme dry conditions, c), and the corresponding anomaly (blue line).

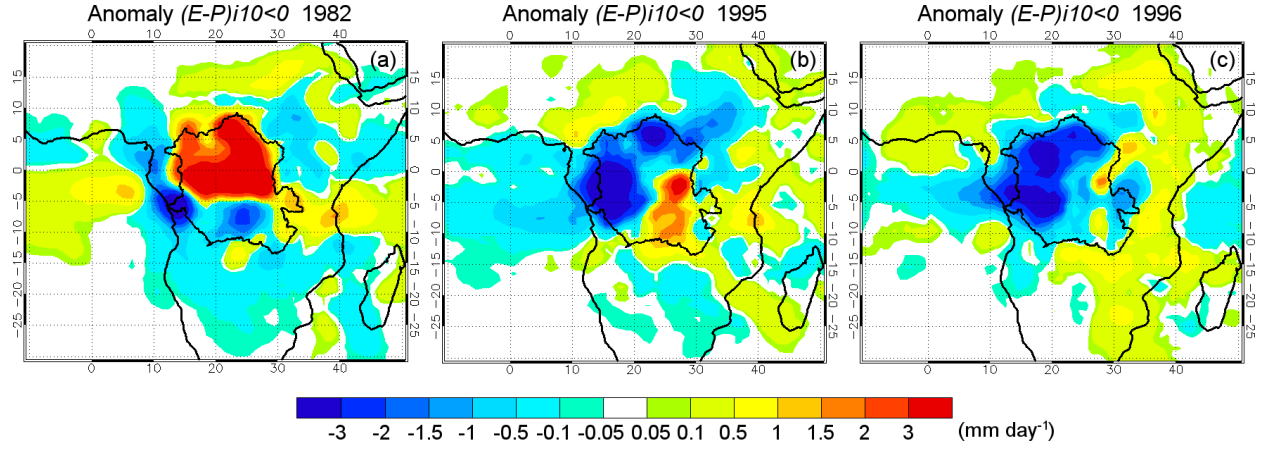

Figure 15. Anomaly of the $|(E-P)i10<0|$ (mm day^{-1}) integrated forwards from the Congo River basin itself during 1982 (severe wet year, a), 1995 (severe dry year, b) and 1996 (extreme dry year, c).